

# Error-Mitigated Hamiltonian Simulation: Complexity Analysis and Optimization for Near-Term and Early-Fault-Tolerant Quantum Computers

Keisuke Murota,<sup>1,\*</sup> Synge Todo,<sup>1,2,3,†</sup> and Suguru Endo<sup>4,5,‡</sup>

<sup>1</sup>*Department of Physics, The University of Tokyo, Tokyo 113-0033, Japan*

<sup>2</sup>*Institute for Physics of Intelligence, The University of Tokyo, Tokyo 113-0033, Japan*

<sup>3</sup>*Institute for Solid State Physics, The University of Tokyo, Kashiwa, 277-8581, Japan*

<sup>4</sup>*NTT Computer and Data Science Laboratories, NTT Inc., Musashino 180-8585, Japan*

<sup>5</sup>*NTT Research Center for Theoretical Quantum Information,  
NTT Inc. 3-1 Morinosato Wakanomiyu, Atsugi, Kanagawa, 243-0198, Japan*

Simulating real-time dynamics under a Hamiltonian is a central goal of quantum information science. While numerous Hamiltonian-simulation quantum algorithms have been proposed, the effects of physical noise have rarely been incorporated into performance analysis, despite the non-negligible noise levels in quantum devices. In this work, we analyze noisy Hamiltonian simulation with quantum error mitigation for Trotterized and randomized LCU-based Hamiltonian simulation algorithms. We give an end-to-end comprehensive complexity analysis of error-mitigated Hamiltonian simulation algorithms using the mean-squared error. Because quantum error mitigation incurs an exponential cost with the number of layers in quantum algorithms, there is a trade-off between the sampling cost and the bias in simulation accuracy or the algorithmic sampling overhead. Optimizing this trade-off, we derive an analytic depth-selection rule and characterize the optimal end-to-end scaling as a function of target accuracy and noise parameters. We further quantify the noise-characterization cost required for error mitigation via gate set tomography and the recently proposed space-time noise inversion method, showing that the latter can significantly reduce the characterization overhead.

## I. INTRODUCTION

Hamiltonian simulation algorithms to simulate the real-time evolution  $e^{-iHt}$  for a Hamiltonian  $H$  are at the center of the quantum computing field, as simulating quantum systems such as condensed matter and chemistry systems is a key goal for quantum computers [1–3]. In addition, Hamiltonian simulation underlies many quantum algorithms, e.g., quantum phase estimation [4–7], a general-dynamics quantum simulator based on the linear combination of Hamiltonian simulation [8, 9], and even a linear system solver [10–12].

The improvement of Hamiltonian simulation complexity has been of significant interest in the quantum computing field. However, while noise is inherently present and cannot be ignored in practice, its impact is frequently underestimated or overlooked in the design of Hamiltonian simulation algorithms. Nevertheless, some works rigorously consider the effect of noise [13–17]. Knee and Munro [13] point out that there is a trade-off relationship between the Trotter count and the physical noise effect in the Trotter-based Hamiltonian simulation, and explicitly show the existence of an optimal Trotter count. While extrapolation-based quantum error mitigation can help overcome this trade-off [14–16], a comprehensive complexity analysis is still missing, except for the second-order Trotter formula [15].

In the present work, we first discuss the complexity of error-mitigated Hamiltonian simulation, incorporating

the effects of physical noise and quantum error mitigation [18–23]. As a QEM method, we mainly discuss the probabilistic error cancellation (PEC) method [19, 20]. PEC inverts the noise effect based on the characterized noise model in advance. Note that the PEC method allows us to compute the sampling overhead and the maximum bias in QEM in an analytical form. We then use the mean-squared error (MSE), denoted by  $\epsilon^2$ , as a performance metric for the error-mitigated Hamiltonian simulation algorithms, because it can reflect both the QEM sampling overhead and the bias [21, 24]. Finally, we minimize the MSE by optimizing the algorithmic depth.

We consider two types of Hamiltonian simulation algorithms suitable for near-term quantum simulation: general product formula [25, 26] and single-ancilla LCU-based simulation algorithms [12]. For Trotterized simulation, we identify two distinct accuracy regimes in the end-to-end sampling cost: a regime where the cost grows only polynomially as the target accuracy becomes small, and a regime where it grows exponentially. This transition implies the existence of a critical error  $\epsilon_c$ , below which pushing the accuracy further becomes prohibitively expensive in terms of the required number of samples. Furthermore, compared with the noisy Trotter-based simulation, combining higher-order product formulas with PEC leads to a *qualitative* improvement in the critical error (the noise-limited precision): the dependence on the effective noise strength improves from a sublinear scaling to a  $k$ th-power scaling for an order- $k$  product formula, corresponding to an exponent improvement by a factor of  $k+1$ . Note that this analysis is directly applicable to the qDrift algorithm because almost the same trade-off holds between the algorithmic and physical errors as for the first-order Trotter formula [27]. For the randomized LCU-based algorithm,

\* keisuke.murota@phys.s.u-tokyo.ac.jp

† wistaria@phys.s.u-tokyo.ac.jp

‡ suguru.endo@ntt.com

we first show that the circuit depth is a random variable with a bounded mean. Therefore, the additional depth needed to improve the simulation accuracy is practically negligible, and the overall performance is dominated by sampling overhead rather than systematic algorithmic bias. When combined with QEM, we further optimize the repetition parameter, which yields a square-root improvement in the dominant time dependence appearing in the exponential sampling overhead compared with a standard (non-optimized) parameter choice.

Finally, we quantify the sampling overhead required for noise characterization when implementing error mitigation, and we assess how the recently introduced space-time noise inversion (SNI) method [28] can improve the scaling of this characterization cost in the early FTQC era. While the SNI method incurs a slight increase in the QEM sampling overhead, we show that a similar optimization strategy is also applicable to the SNI method, with significantly improved characterization cost.

## II. HAMILTONIAN SIMULATION ALGORITHMS

Here, we summarize the two Hamiltonian-simulation algorithms that will be used throughout the paper. We consider an  $n$ -qubit Hamiltonian  $H$  and a simulation time  $t > 0$ . We assume throughout that the Hamiltonian admits a Pauli expansion

$$H = \sum_{\ell=1}^L \lambda_{\ell} P_{\ell}, \quad (1)$$

where each  $P_{\ell}$  is a Pauli string and  $\lambda_{\ell} \in \mathbb{R}$ . This representation is always available for qubit Hamiltonians. We assume that each Pauli rotation  $e^{-i\lambda_{\ell} P_{\ell} \delta}$  can be implemented for any step size  $\delta$ . For notational convenience, we also write  $H = \sum_{\ell=1}^L H_{\ell}$  by setting  $H_{\ell} := \lambda_{\ell} P_{\ell}$ . In this convention,  $L$  denotes the number of Pauli terms in the Hamiltonian  $H$ .

### A. First-order Trotter: baseline bias

Let  $t > 0$  denote the evolution time. Our target unitary channel and expectation value are

$$\mathcal{U}_t(\rho) = e^{-iHt} \rho e^{+iHt}, \quad \mu = \text{Tr}[O \mathcal{U}_t(\rho)], \quad (2)$$

where we assume  $\|O\|_{\infty} \leq 1$  (otherwise rescale  $O$ ).

Let  $N \in \mathbb{N}$  be the number of Trotter layers and set  $\delta = t/N$ . Define the first-order (Trotter) microstep unitary and its channel as

$$S_1(\delta) := \prod_{\ell=1}^L e^{-iH_{\ell}\delta}, \quad \mathcal{S}_{1,\delta}(\rho) := S_1(\delta) \rho S_1(\delta)^{\dagger}. \quad (3)$$

The  $N$ -step Trotter channel is given by the composition

$$\mathcal{V}_N^{(1)} := (\mathcal{S}_{1,\delta})^N. \quad (4)$$

We estimate  $\mu$  by  $\hat{\mu}$  whose mean is  $\mathbb{E}[\hat{\mu}] = \text{Tr}[O \mathcal{V}_N^{(1)}(\rho)]$ .

*Bias described by the channel trace distance* – Throughout this paper, we use the diamond distance to characterize the bias in the Hamiltonian simulation algorithms.

$$\|\Phi - \Psi\|_{\diamond} := \max_{\rho} \|(\Phi \otimes \text{id})(\rho) - (\Psi \otimes \text{id})(\rho)\|_1, \quad (5)$$

where  $\|\cdot\|_1$  denotes the trace norm. We here denote  $D(\Phi, \Psi) = \frac{1}{2} \|\Phi - \Psi\|_{\diamond}$ . We can alternatively use the induced trace distance  $D_{\text{IT}}(\Phi, \Psi) := \frac{1}{2} \max_{\rho} \|\Phi(\rho) - \Psi(\rho)\|_1$ , where the maximization is over density operators  $\rho$ . These distance measures obey the triangle inequality and are contractive under composition with CPTP maps: for any CPTP map  $\Lambda$ ,

$$\begin{aligned} D(\Lambda \circ \Phi, \Lambda \circ \Psi) &\leq D(\Phi, \Psi), \\ D(\Phi \circ \Lambda, \Psi \circ \Lambda) &\leq D(\Phi, \Psi). \end{aligned} \quad (6)$$

In particular, for any state  $\rho$  and any observable  $O$  with  $\|O\|_{\infty} \leq 1$ ,

$$|\text{Tr}[O\mathcal{A}(\rho)] - \text{Tr}[O\mathcal{B}(\rho)]| \leq D(\mathcal{A}, \mathcal{B}). \quad (7)$$

Then the algorithmic bias satisfies

$$|\mathbb{E}[\hat{\mu}] - \mu| \leq D(\mathcal{U}_t, \mathcal{V}_N^{(1)}). \quad (8)$$

Note that, while the induced trace distance measure gives a tighter bound on the bias of the expectation values than the diamond norm distance, the QEM sampling overhead can be systematically bounded by using the diamond norm distance as we will show later. Therefore, we mainly use the diamond norm distance measure.

*A commutator bound for the first-order step* – We can bound the first-order Trotter error by using commutators. In particular, Childs *et al.* [26] prove a tight additive-error bound for the first-order Trotter formula:

$$\|S_1(t) - e^{-iHt}\| \leq \frac{t^2}{2} \sum_{\ell=1}^L \left\| \left[ \sum_{m>\ell} H_m, H_{\ell} \right] \right\|. \quad (9)$$

Here  $\|\cdot\|$  is the operator norm. Applying (9) to one microstep of size  $\delta$  and using  $\delta = t/N$ , we obtain a per-step bound  $\|S_1(\delta) - e^{-iH\delta}\| \leq c_1 \delta^2$  with the explicit prefactor

$$c_1 := \frac{1}{2} \sum_{\ell=1}^L \left\| \left[ \sum_{m>\ell} H_m, H_{\ell} \right] \right\|. \quad (10)$$

For unitary channels one has  $D(\mathcal{A}, \mathcal{B}) \leq \|A - B\|$ , so  $D(\mathcal{S}_{1,\delta}, \mathcal{U}_{\delta}) \leq c_1 \delta^2$ . The triangle inequality and contractivity of  $D$  over  $N$  steps then give

$$D(\mathcal{U}_t, \mathcal{V}_N^{(1)}) \leq N c_1 \delta^2 = \frac{c_1 t^2}{N}. \quad (11)$$

It is convenient to package the  $t$ -dependence into the first-order Trotter constant

$$\alpha_1 := c_1 t^2, \quad D(\mathcal{U}_t, \mathcal{V}_N^{(1)}) \leq \frac{\alpha_1}{N}. \quad (12)$$

Thus, at fixed Hamiltonian decomposition, the algorithmic bias decays as  $O(1/N)$  with an explicit commutator-controlled prefactor  $\alpha_1$ .

### B. Higher-order Suzuki–Trotter product formulas and commutator scaling

We now consider even-order Suzuki–Trotter formulas. Write  $N$  for the number of repeated *microsteps* and set  $\delta = t/N$ .

*Recursive construction for order  $k = 2p$  for an integer  $p \geq 1$*  – We start by defining the second-order microstep channel

$$\begin{aligned} \mathcal{S}_{2,\delta}(\rho) := & \left( \prod_{\ell=1}^L e^{-iH_\ell \frac{\delta}{2}} \right) \left( \prod_{\ell=L}^1 e^{-iH_\ell \frac{\delta}{2}} \right) \rho \\ & \times \left( \prod_{\ell=1}^L e^{+iH_\ell \frac{\delta}{2}} \right) \left( \prod_{\ell=L}^1 e^{+iH_\ell \frac{\delta}{2}} \right), \end{aligned} \quad (13)$$

and the depth- $N$  channel  $\mathcal{V}_N^{(2)} := (\mathcal{S}_{2,\delta})^N$ . For even orders  $k = 2p \geq 4$ , we recursively define the microstep channel

$$\begin{aligned} \mathcal{S}_{k,\delta} := & \frac{\mathcal{S}_{k-2, u_p \delta}^2 \mathcal{S}_{k-2, (1-4u_p)\delta} \mathcal{S}_{k-2, u_p \delta}^2}{1} \\ u_p = & \frac{1}{4 - 4^{1/(2p-1)}}. \end{aligned} \quad (14)$$

The corresponding channel is

$$\mathcal{V}_N^{(k)} := (\mathcal{S}_{k,\delta})^N, \quad (15)$$

with  $\delta = t/N$ .

*Commutator-controlled prefactors* – Following Childs *et al.* [26], the global Trotter error for order  $k$  satisfies  $D(\mathcal{U}_t, \mathcal{V}_N^{(k)}) \leq O(\alpha_{\text{comm}} t^{k+1}/N^k)$ , where  $\alpha_{\text{comm}}$  is the prefactor defined as

$$\alpha_{\text{comm}} := \sum_{\ell_1, \dots, \ell_{k+1}=1}^L \left\| [H_{\ell_{k+1}}, \dots, [H_{\ell_2}, H_{\ell_1}] \dots] \right\|. \quad (16)$$

Each  $k$ th-order microstep  $\mathcal{S}_{k,\delta}$ , however, unfolds recursively into  $\Upsilon_k = 2 \times 5^{k/2-1}$  stages, so the total number of circuit layers is  $d = \Upsilon_k N$ . Thus the bound can be rewritten as

$$D(\mathcal{U}_t, \mathcal{V}_N^{(k)}) \leq \frac{\alpha_k}{d^k}, \quad (17)$$

where  $\alpha_k = O(\Upsilon_k^k \alpha_{\text{comm}} t^{k+1})$ . For geometrically local Hamiltonians,  $\alpha_{\text{comm}} = O(L)$ , because each term  $H_\ell$  commutes with all but  $O(1)$  neighbors, causing most nested commutators to vanish [26]. Note that Eq. (17) and the definition of  $\alpha_{\text{comm}}$  encompass the first-order case as a special instance, where we define  $\Upsilon_1 = 1$ , i.e.  $\alpha_1 = O(\alpha_{\text{comm}} t^2)$  as in Eq. (12).

### C. Randomized linear combination of unitaries for real-time simulation

Here, we review the recently introduced randomized linear combination of unitaries (RLCU) algorithm for real-time simulation [12]. Because this algorithm uses a random sampling of gates, it is convenient to introduce the normalized Hamiltonian

$$\tilde{H} := \frac{H}{\beta} = \sum_{s=1}^L p_s P_s, \quad (18)$$

where  $\beta = \sum_{s=1}^L |\lambda_s|$ ,  $p_s := \frac{|\lambda_s|}{\beta}$ . We also introduce the scaled time as  $\tilde{t} := \beta t$ . We measure the gate count in a gate model where a Pauli rotation  $e^{-i\theta P_s}$  is treated as one elementary operation. We approximate the segment evolution  $e^{-iHt/r}$  by the (truncated) Taylor expansion [2, 7]

$$S_r := \sum_{k=0}^K \frac{(-itH/r)^k}{k!} = \sum_{k=0}^K \frac{(-i\tilde{t}\tilde{H}/r)^k}{k!}, \quad (19)$$

and later repeat this segment  $r$  times to approximate  $e^{-iHt}$ . Originally, a finite cutoff parameter  $K$  was introduced in the Taylor expansion to truncate the infinite series. In this work, however, we take the limit  $K \rightarrow \infty$  and retain the full Taylor series. As we explain below, sampling from the resulting infinite summation can be performed efficiently.

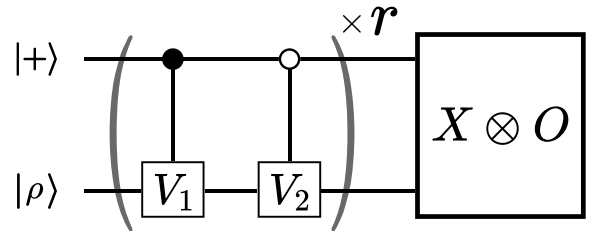


FIG. 1: Quantum circuit for implementing the linear map  $(S_r)^r = (\sum_\mu \alpha_\mu U_\mu)^r$  and measuring an observable  $O$  against an input state  $\rho$ , using the RLCU algorithm.

We randomly sample  $V_1$  and  $V_2$  according to the probability distribution  $\{\alpha_\mu / \|\alpha\|_1, U_\mu\}$ , where  $\|\alpha\|_1 = \sum_\mu |\alpha_\mu|$ .

*LCU decomposition of one segment  $S_r$*  – Let  $\lambda := \tilde{t}/r$ . We group the Taylor-series terms by pairing even and odd

orders:

$$\begin{aligned}
\tilde{S}_r &:= \sum_{k=0}^{\infty} \frac{(-i\tilde{t}\tilde{H}/r)^k}{k!} \\
&= \sum_{k \in \text{even}}^{\infty} \frac{1}{k!} \left(-\frac{i\tilde{t}}{r}\tilde{H}\right)^k \left(I - \frac{i\tilde{t}\tilde{H}/r}{k+1}\right) \\
&= \sum_{k \in \text{even}}^{\infty} \frac{(-i\tilde{t}/r)^k}{k!} \sqrt{1 + \left(\frac{\tilde{t}/r}{k+1}\right)^2} \\
&\quad \times \sum_{\ell_1, \ell_2, \dots, \ell_k, m}^L p_{\ell_1} \cdots p_{\ell_k} p_m P_{\ell_1} \cdots P_{\ell_k} e^{-i\theta_k P_m}.
\end{aligned} \tag{20}$$

where  $\theta_k$  is chosen so that

$$e^{-i\theta_k P_m} = \frac{I - i\frac{\lambda}{k+1}P_m}{\sqrt{1 + \left(\frac{\lambda}{k+1}\right)^2}}. \tag{21}$$

Thus  $S_r$  is written as an LCU:

$$S_r = \sum_{\mu} \alpha_{\mu} U_{\mu}, \tag{22}$$

where we may take the multi-index  $\mu = (k, \ell_1, \dots, \ell_k, m)$  with even  $k$ , and define

$$U_{(k, \ell, m)} := P_{\ell_1} \cdots P_{\ell_k} e^{-i\theta_k P_m}, \tag{23}$$

and the corresponding nonnegative coefficient

$$\alpha_{(k, \ell, m)} := \frac{\lambda^k}{k!} \sqrt{1 + \left(\frac{\lambda}{k+1}\right)^2} \left(\prod_{j=1}^k p_{\ell_j}\right) p_m. \tag{24}$$

The 1-norm of the LCU coefficients is then

$$\|\alpha\|_1 := \sum_{\mu} \alpha_{\mu} = \sum_{k \in \text{even}}^{\infty} \frac{\lambda^k}{k!} \sqrt{1 + \left(\frac{\lambda}{k+1}\right)^2}, \tag{25}$$

where we used  $\sum_{\ell_1, \dots, \ell_k, m} (\prod_j p_{\ell_j}) p_m = 1$ .

*Sampling procedure and estimator* To estimate the expectation value  $\text{Tr}[O(S_r)^r(\rho)]$  for an observable  $O$  and input state  $\rho$ , we proceed as follows. We initialize the joint ancilla–system state as  $|+\rangle\langle+| \otimes \rho$  and apply the circuit in Fig. 1 for  $r$  rounds. In each round  $j \in \{1, \dots, r\}$ , we independently sample two unitaries  $V_{1, \nu}$  and  $V_{2, \mu}$  from the distribution  $\{p_{\mu}, U_{\mu}\}$ , where

$$p_{\mu} := \frac{\alpha_{\mu}}{\|\alpha\|_1}, \tag{26}$$

with the total (algorithmic) sampling overhead being  $\Gamma_{\text{RLCU}} := (\Gamma_S)^r$ . We call  $\Gamma_S := \|\alpha\|_1^2$  the segment sampling overhead. In practice, sampling from the infinite series can be carried out by first drawing the Taylor order  $k$  from an even-Poisson distribution and then applying thinning to obtain a sample from  $p(k, \lambda)$ , followed by

selecting each Pauli string  $P_{\ell}$  independently according to the discrete distribution  $\{p_{\ell}\}$ . On average, this random process implements the microstep channel  $\tilde{S}_r$  at the channel level. For each sampled pair  $(U_{\mu}, U_{\nu})$ , we define the joint ancilla–system gate

$$G_{\mu\nu} := |0\rangle\langle 0|_A \otimes U_{\nu} + |1\rangle\langle 1|_A \otimes U_{\mu}, \tag{27}$$

which applies  $U_{\nu}$  when the ancilla is in  $|0\rangle$  and  $U_{\mu}$  when it is in  $|1\rangle$ . The averaged channel is

$$\tilde{S}_r(\sigma) := \sum_{\mu, \nu} p_{\mu} p_{\nu} G_{\mu\nu} \sigma G_{\mu\nu}^{\dagger} \tag{28}$$

for any density matrix  $\sigma$  on the joint ancilla–system space. After  $r$  rounds, we measure  $X \otimes O$  on the final state and scale by  $\Gamma_{\text{RLCU}}$ . The  $|+\rangle$  state is preserved in the ancilla throughout, and measuring  $X \otimes O$  followed by reweighting by  $\Gamma_{\text{RLCU}}$  gives the unbiased estimator of  $\text{Tr}[O(S_r)^r(\rho)]$ :

$$\begin{aligned}
&\Gamma_{\text{RLCU}} \text{Tr}\left[(X \otimes O) \tilde{S}_r^r(|+\rangle\langle+| \otimes \rho)\right] \\
&= \Gamma_{\text{RLCU}} \text{Tr}\left[O\left(\sum_{\mu} p_{\mu} U_{\mu}\right)^r \rho \left(\sum_{\nu} p_{\nu} U_{\nu}^{\dagger}\right)^r\right] \\
&= \text{Tr}\left[O S_r^r \rho (S_r^r)^{\dagger}\right].
\end{aligned} \tag{29}$$

Here, we used the definition of  $\Gamma_{\text{RLCU}} = \|\alpha\|_1^{2r}$  and Eq. (22) to obtain the last line. Denoting the measured outcome by  $\hat{\nu}$ , the unbiased estimator is

$$\hat{\mu}_r := \Gamma_{\text{RLCU}} \frac{1}{M} \sum_{j=1}^M \hat{\nu}_j, \tag{30}$$

where  $M$  is the number of circuit repetitions. The reweighting by  $\Gamma_{\text{RLCU}}$  amplifies statistical fluctuations by a factor  $\Gamma_{\text{RLCU}}^2$ . Because  $\text{Var}\left(\frac{1}{M} \sum_{j=1}^M \hat{\nu}_j\right) = \text{Var}(\hat{\nu})/M$  and  $\|\hat{\nu}\|_{\infty} \leq 1$ ,

$$\text{Var}(\hat{\mu}_r) = \Gamma_{\text{RLCU}}^2 \frac{\text{Var}(\hat{\nu})}{M} \leq \frac{\Gamma_{\text{RLCU}}^2}{M}. \tag{31}$$

Chakraborty [12] show that the segment sampling overhead satisfies  $\Gamma_S \leq \exp\left(\frac{\tilde{t}^2}{r^2}\right)$ , and therefore the total sampling overhead is bounded by

$$\Gamma_{\text{RLCU}} \leq \exp\left(\frac{\tilde{t}^2}{r}\right). \tag{32}$$

*Expected number of Clifford gates and variance* – An important feature of the RLCU algorithm is that the number of Clifford gates per segment is a random variable determined by the sampled Taylor order  $k$ . We now bound the expected number of Clifford gates and its variance, both of which will be used in the analysis of the QEM sampling overhead in later sections.

**Theorem 1** (Average and variance of the number of Clifford gates). *Let  $\lambda := t/r = \beta t/r$ , and let  $p(k, \lambda)$  denote the probability that the RLCU algorithm samples Taylor order  $k$  in a single segment. Then the mean and variance of the number of Clifford gates satisfy*

$$\mathbb{E}_p[k] \leq \lambda \tanh(\lambda) \leq \lambda^2, \quad (33)$$

$$\text{Var}_p(k) := \mathbb{E}_p[k^2] - \mathbb{E}_p[k]^2 \leq \lambda^2 + \lambda \tanh(\lambda) \leq 2\lambda^2. \quad (34)$$

The proof is given in Appendix B.

### III. OPTIMAL NUMBER OF LAYERS WITH THE PRESENCE OF PHYSICAL NOISE FOR TROTTER-BASED ALGORITHMS AND RANDOMIZED LCU-BASED ALGORITHMS

In a noisy quantum device, increasing the circuit depth reduces the algorithmic approximation error but simultaneously accumulates physical noise. This creates a fundamental trade-off that determines the optimal depth for each algorithm. In this section, we analyze this trade-off for both the Suzuki–Trotter and randomized LCU algorithms, and identify the optimal depth that minimizes the mean-squared error (MSE).

#### A. Suzuki–Trotter-based algorithm

We first analyze the Suzuki–Trotter algorithm under physical noise. We quantify this trade-off by bounding the total distance between the ideal evolution and the noisy Trotter channel, using the properties of the diamond distance defined in section II A. The noisy channel of each Trotter step is

$$\mathcal{E}_\delta^{\text{noisy}} = \prod_{\ell=1}^L \mathcal{N}_\ell \mathcal{U}_\delta^\ell, \quad (35)$$

where  $\mathcal{U}_\delta^\ell$  denotes the unitary channel corresponding to the  $\ell$ -th elementary operation (i.e., the Pauli rotation gate) and  $\mathcal{N}_\ell$  is the noise process associated with the  $\ell$ -th elementary operation. The distance between the noise-free ideal channel and the noisy channel is

$$\begin{aligned} D(\mathcal{U}_\delta, \mathcal{E}_\delta^{\text{noisy}}) &\leq D(\mathcal{U}_\delta, \mathcal{S}_{k,\delta}) + D(\mathcal{S}_{k,\delta}, \mathcal{E}_\delta^{\text{noisy}}) \\ &\leq D(\mathcal{U}_\delta, \mathcal{S}_{k,\delta}) + \sum_{\ell=1}^L D(\mathcal{N}_\ell \circ \mathcal{U}_\delta^\ell, \mathcal{U}_\delta^\ell) \\ &= D(\mathcal{U}_\delta, \mathcal{S}_{k,\delta}) + \sum_{\ell=1}^L D(\mathcal{N}_\ell, \mathcal{I}), \end{aligned} \quad (36)$$

where  $\mathcal{S}_{k,\delta}$  denotes the channel for one layer of the order- $k$  Trotter formula and we use the triangle inequality and the contractivity Eq. (6). Therefore, for the  $k$ th-order

Suzuki–Trotter algorithm, the total distance between the ideal channel  $\mathcal{U}_t$  and the noisy channel  $(\mathcal{E}_\delta^{\text{noisy}})^d$  is

$$\begin{aligned} D(\mathcal{U}_t, (\mathcal{E}_\delta^{\text{noisy}})^d) &\leq d D(\mathcal{U}_\delta, \mathcal{E}_\delta^{\text{noisy}}) \\ &\leq \frac{\alpha_k}{d^k} + Ld\gamma, \end{aligned} \quad (37)$$

with  $\gamma := \max_\ell D(\mathcal{N}_\ell, \mathcal{I})$ , which we call the per-gate error. We used Eq. (17) to bound the algorithmic bias. For a normalized observable  $O$  with  $\|O\|_\infty \leq 1$ , the bias satisfies  $|\text{Tr}[O\mathcal{U}_t(\rho_{\text{in}})] - \text{Tr}[O(\mathcal{E}_\delta^{\text{noisy}})^d(\rho_{\text{in}})]| \leq D(\mathcal{U}_t, (\mathcal{E}_\delta^{\text{noisy}})^d)$ . Therefore, we can upper-bound the bias of the expectation value by  $\frac{\alpha_k}{d^k} + Ld\gamma$ .

We evaluate the performance of the noisy Hamiltonian simulation using the mean-squared error (MSE). Refer to Appendix A for the basic properties of MSE. In this work, the MSE plays the role of a unified error metric that captures both systematic error and sampling error in a single quantity: the squared bias represents a consistent deviation from the ideal value (e.g., from algorithmic approximation and physical noise), while the variance represents random fluctuations due to a finite number of samples. Accordingly, targeting a small MSE simultaneously controls these two contributions. See Appendix A for a simple conservative confidence-interval interpretation. The MSE is defined as

$$\epsilon^2 = \text{Var}(\hat{\mu}) + \text{Bias}(\hat{\mu})^2. \quad (38)$$

In this paper, we call  $\epsilon$ , the square root of the MSE, the error or accuracy. Using Eq. (37) and assuming that we use  $M$  samples to estimate the expectation value, we obtain the bound:

$$\epsilon^2 \leq \left(\frac{\alpha_k}{d^k} + Ld\gamma\right)^2 + \frac{1}{M}. \quad (39)$$

We recall that the observable is normalized so that  $\|O\|_\infty \leq 1$ . If needed, rescale to satisfy  $\|O\|_\infty \leq 1$ , then the variance scales as  $O(1/M)$ . We can minimize the MSE in Eq. (39) by optimizing  $d$  and obtain the optimized error bound

$$\epsilon^{2*} = (C_k \alpha_k^{1/(k+1)} (L\gamma)^{k/(k+1)})^2 + \frac{1}{M}. \quad (40)$$

Here,  $C_k = (k^{1/(k+1)} + k^{-k/(k+1)})$  is a constant that depends on the order  $k$ . Because the first term in Eq. (40) is independent of  $M$ , the MSE cannot be reduced below it by increasing the number of samples. We refer to the first term in Eq. (40) as the *error bound* for Suzuki–Trotter simulation without PEC and denote it as  $\epsilon_b$ . Using the scaling  $\alpha_k = O(t^{k+1}L)$  for geometrically local Hamiltonians, the error bound scales as  $O(tL(\gamma)^{k/(k+1)})$ . Interestingly, without any error mitigation, the error bound always scales at least linearly in both  $t$  and  $L$ , and the exponent of  $\gamma$  satisfies  $k/(k+1) < 1$  for any finite  $k$ , so the noise dependence remains sublinear in  $\gamma$ .

## B. Randomized LCU-based algorithm

We next analyze the randomized linear combination of unitaries (RLCU) algorithm under physical noise. In contrast to product formulas, in the  $K \rightarrow \infty$  limit the ideal segment operator satisfies  $S_r = e^{-iHt/r}$  and hence  $(S_r)^r = e^{-iHt}$ . Therefore, in the absence of physical noise, the estimator  $\hat{\mu}_r$  in Eq. (30) is unbiased for  $\mu = \text{Tr}[OU_t(\rho)]$ , at the cost of the sampling overhead  $\Gamma_{\text{RLCU}}$ . With physical noise, the implemented channel becomes random because the circuit depth per segment is a random variable determined by the sampled Taylor order.

To correctly evaluate the bias, we first express the RLCU process using Eq. (28). The channel corresponding to the gate  $G_{\mu\nu}$  in Eq. (27) is denoted by  $\mathcal{G}_{\mu\nu}(\sigma) := G_{\mu\nu} \sigma G_{\mu\nu}^\dagger$ . We write this channel as

$$\mathcal{G}_{\mu\nu} = \mathcal{G}_{1,\mu} \mathcal{G}_{2,\nu} = \left( \prod_{\ell=1}^{L_\mu} \mathcal{G}_\mu^\ell \right) \left( \prod_{\ell=1}^{L_\nu} \mathcal{G}_\nu^\ell \right), \quad (41)$$

where  $\mathcal{G}_{1,\mu}$  and  $\mathcal{G}_{2,\nu}$  are the channels corresponding to the two control unitaries in fig. 1, and  $\mathcal{G}_\mu^\ell$  denotes the  $\ell$ -th elementary gate when the realization  $\mathcal{G}_{1,\mu}$  is decomposed into elementary operations. In our gate model,  $L_\mu = 1 + k_\mu$  where  $k_\mu$  is the Taylor order for the sampled  $\mu$ . The noisy channel for  $\mathcal{G}_{1,\mu}$  is

$$\mathcal{E}_\mu^{\text{noisy}} := \prod_{\ell=1}^{L_\mu} \mathcal{N}_\ell \circ \mathcal{G}_\mu^\ell, \quad (42)$$

where  $\mathcal{N}_\ell$  is the noise process associated with the  $\ell$ th elementary operation. The distance between the ideal channel  $\mathcal{G}_\mu$  and the noisy channel satisfies

$$D(\mathcal{G}_\mu, \mathcal{E}_\mu^{\text{noisy}}) \leq \sum_{\ell=1}^{L_\mu} D(\mathcal{N}_\ell, \mathcal{I}) \leq \gamma + \gamma_c k_\mu, \quad (43)$$

where  $\gamma$  is the maximum per-gate error for non-Clifford gates,  $\gamma_c$  is that for Clifford gates, and  $k_\mu$  is the Taylor order for the realization  $\mu$ . Taking the expectation over the algorithmic randomness and using  $\mathbb{E}[k] \leq (\beta t/r)^2$  from theorem 1, we obtain  $\mathbb{E}[D(\mathcal{G}_\mu, \mathcal{E}_\mu^{\text{noisy}})] \leq \gamma + \gamma_c (\beta t/r)^2$  per segment. Therefore, denoting the noisy stroboscopic channel of  $\tilde{\mathcal{S}}_r$  by  $\tilde{\mathcal{E}}_r^{\text{noisy}}$ , the distance between the ideal and noisy segment channels satisfies

$$D(\tilde{\mathcal{S}}_r, \tilde{\mathcal{E}}_r^{\text{noisy}}) \leq 2 \left( \gamma + \gamma_c \frac{(\beta t)^2}{r^2} \right). \quad (44)$$

Repeating this segment  $r$  times, the total bias accumulates to  $r$  times the per-segment distance. Because the RLCU estimator is reweighted by  $\Gamma_{\text{RLCU}}$  (see Eq. (30)), the bias is amplified by the same factor and becomes

$$\text{Bias}(\hat{\mu}_r) = |\mathbb{E}[\hat{\mu}_r] - \mu| \leq \Gamma_{\text{RLCU}} \cdot 2 \left( \gamma r + \gamma_c \frac{(\beta t)^2}{r} \right), \quad (45)$$

where  $\Gamma_{\text{RLCU}} \leq \exp((\beta t)^2/r)$ . Combining the bias bound with the variance bound in Eq. (31), we obtain

$$\epsilon^2 \leq \frac{\exp(2(\beta t)^2/r)}{M} + \left( 2e^{(\beta t)^2/r} \cdot (\gamma r + \gamma_c \frac{(\beta t)^2}{r}) \right)^2. \quad (46)$$

It is not straightforward to analytically optimize the MSE with respect to  $r$ . However, because the variance term can be reduced by increasing  $M$  but the bias term cannot, we can still obtain the *error bound* for the randomized LCU algorithm. The leading contribution to the bias scales as  $b(r) \sim e^{(\beta t)^2/r} \cdot (\gamma r + \gamma_c \frac{(\beta t)^2}{r})$ . Optimizing  $b(r)$  with respect to  $r$ , the stationary condition  $\partial_r b = 0$  yields  $r^3 - (\beta t)^2 r^2 - (\gamma_c/\gamma)(\beta t)^2 r - (\gamma_c/\gamma)(\beta t)^4 = 0$ . In the regime  $\gamma_c \ll \gamma$ , the  $(\gamma_c/\gamma)$  terms are negligible, and hence  $r^* \approx (\beta t)^2$ . At this choice, the error bound scales as  $\epsilon_b \sim O(\gamma(\beta t)^2)$ , i.e.  $O(\gamma)$  with respect to the per-gate error  $\gamma$  and quadratically with respect to time-space volume  $\beta t$ .

## IV. PROBABILISTIC ERROR CANCELLATION

The analysis in the previous section reveals fundamental limits on noisy Hamiltonian simulation: for Trotter algorithms, the error bound  $\epsilon_b$  cannot be reduced below a noise-dependent floor by increasing the number of samples alone. To overcome these limitations, we now review the probabilistic error cancellation (PEC) method [19, 20], a quantum error mitigation technique that suppresses physical errors at the cost of increased sampling overhead.

Suppose that a noisy quantum circuit can be described by  $\prod_{k=1}^{N_G} \mathcal{N}_k \mathcal{U}_k$ , where  $\mathcal{U}_k$  denotes the  $k$ th ideal gate channel,  $\mathcal{N}_k$  its associated noise, and  $N_G$  is the total number of gates. In PEC, the noise model is characterized in advance. Based on this information, we construct an approximate inverse map via a quasiprobability decomposition  $\mathcal{N}_k^{-1} = \sum_{i_k} q_{i_k} \mathcal{B}_{i_k}$ , where  $q_{i_k} \in \mathbb{R}$  and  $\mathcal{B}_{i_k}$  are implementable basis operations. Then we can represent the ideal channel  $\mathcal{U}_{\text{id}} = \prod_{k=1}^{N_G} \mathcal{U}_k$  as

$$\begin{aligned} \mathcal{U}_{\text{id}} &= \prod_{k=1}^{N_G} \sum_{i_k} q_{i_k} \mathcal{B}_{i_k} \mathcal{N}_k \mathcal{U}_k \\ &= \Gamma \sum_{i_1, i_2, \dots, i_{N_G}} \prod_{k=1}^{N_G} p_{i_k} \text{sgn}(q_{i_k}) \mathcal{B}_{i_k} \mathcal{N}_k \mathcal{U}_k, \end{aligned} \quad (47)$$

with  $\Gamma = \prod_{k=1}^{N_G} \Gamma_k$ ,  $\Gamma_k = \sum_{i_k} |q_{i_k}|$  and  $p_{i_k} = |q_{i_k}|/\Gamma_k$ . For simplicity, consider the case where each gate is affected by the same noise.

For an observable  $O$  and input state  $\rho$ , the error-canceled expectation value is given by

$$\begin{aligned} \text{Tr}[O \mathcal{U}_{\text{id}}(\rho)] &= \\ \Gamma \sum_{i_1, i_2, \dots, i_{N_G}} \prod_{k=1}^{N_G} p_{i_k} \text{sgn}(q_{i_k}) &\text{Tr} \left[ \prod_{k=1}^{N_G} \mathcal{B}_{i_k} \mathcal{N}_k \mathcal{U}_k(\rho) O \right]. \end{aligned} \quad (48)$$

Then, the unbiased expectation value can be obtained as follows. We randomly generate the basis operations for QEM  $\mathcal{B}_{i_k}$  with the probability  $p_{i_k}$ , and measure the observable  $O$ , obtaining the random variable  $\hat{\nu} = \prod_{k=1}^{N_G} \text{sgn}(q_{i_k}) \hat{o}$  for the measured outcome  $\hat{o}$ . Finally, we repeat this procedure, with  $\Gamma \langle \hat{\nu} \rangle$  being the unbiased estimator of the noiseless expectation value. Because we need to amplify the random variable with  $\Gamma$ , the variance scales with  $\Gamma^2$ , which scales exponentially with the number of the gates and the error rate.

We now discuss the relationship between the error rate characterized by the distance measure and the PEC sampling cost. For a gate with error rate  $\gamma_k = D(\mathcal{N}_k, \mathcal{I})$ , the optimal sampling cost for implementing  $\mathcal{N}_k^{-1}$  with the completely-positive trace non-increasing basis operations is given by [29, 30]

$$\Gamma_k^{\text{opt}} = \|\mathcal{N}_k^{-1}\|_{\diamond}. \quad (49)$$

Moreover, denoting  $\Delta_k = \mathcal{N}_k - \mathcal{I}$  and since  $\|\Delta_k\|_{\diamond} = 2\gamma_k$ , we have

$$\begin{aligned} \|\mathcal{N}_k^{-1}\|_{\diamond} &= \|(\mathcal{I} - \Delta_k)^{-1}\|_{\diamond} \\ &= \left\| \sum_{m=0}^{\infty} \Delta_k^m \right\|_{\diamond} \leq \frac{1}{1 - 2\gamma_k}, \end{aligned} \quad (50)$$

where we use the triangle inequality as  $\|\sum_{m=0}^{\infty} \Delta_k^m\|_{\diamond} \leq \sum_{m=0}^{\infty} \|\Delta_k\|_{\diamond}^m$  in the last line. Therefore,

$$\Gamma_k^{\text{opt}} \leq \frac{1}{1 - 2\gamma_k}. \quad (51)$$

Because of  $\gamma_k < \gamma$ , this further implies

$$\Gamma^{\text{opt}}(\mathcal{N}_k) \leq \frac{1}{1 - 2\gamma} = 1 + 2\gamma + O(\gamma^2). \quad (52)$$

While the PEC cost depends on the concrete choice of the basis operation, we assume that the per-gate PEC overhead is represented as  $\Gamma_k \leq 1 + \gamma'$ , where  $\gamma' \propto \gamma$  with a proportionality constant that depends on the noise model and the particular quasi-probability decomposition. We then obtain

$$\Gamma = (1 + \gamma')^{N_G} \simeq e^{N_G \gamma'}. \quad (53)$$

## V. OPTIMIZATION OF THE HAMILTONIAN SIMULATION ALGORITHMS UNDER THE USE OF PEC

Having established the PEC formalism, we now combine it with the Hamiltonian simulation algorithms from section III. Because PEC incurs a sampling overhead that grows exponentially with the circuit depth, the optimal depth must now balance three competing factors: algorithmic error, physical noise, and the PEC cost. In the Trotter case, the gate count is  $N_G = dL$ , so the PEC overhead scales as  $\Gamma \simeq e^{Ld\gamma'}$ . Note that we ignore the bias due to the incomplete characterization of noise in this section. We later discuss the required characterization overhead to achieve the target accuracy.

### A. Optimizing the depth of the Trotter-based algorithm under QEM

With PEC, the noise will be completely mitigated at the cost of sampling overhead  $\Gamma = e^{Ld\gamma'}$ .

$$\epsilon(d, M)^2 = \left(\frac{\alpha_k}{d^k}\right)^2 + \frac{e^{2Ld\gamma'}}{M}. \quad (54)$$

The stationary condition  $\partial_d \epsilon(d, M) = 0$  yields

$$M = \frac{L\gamma'}{k \alpha_k^2} e^{2Ld\gamma'} d^{2k+1} \quad (55)$$

Substituting this  $M$  into Eq. (54), the optimal number of layers for a given accuracy  $d(\epsilon)$  can be obtained by solving

$$\epsilon^2 = \frac{\alpha_k^2}{d^{2k}} \left(1 + \frac{k}{\gamma' L d}\right). \quad (56)$$

To derive  $M(\epsilon)$ , we first note that the two terms inside the parentheses of Eq. (56) have distinct origins. The “1” comes from the algorithmic error in the Suzuki–Trotter decomposition, and  $k/(\gamma' L d)$  from the PEC sampling cost. The crossover  $k/(\gamma' L d) = 1$  occurs at  $d = k/(\gamma' L)$ , which upon substitution into Eq. (56) gives  $\epsilon \sim \epsilon_c$  with  $\epsilon_c := \alpha_k (L\gamma'/k)^k$ . For  $\epsilon \ll \epsilon_c$ , the required layer count satisfies  $d \gg k/(\gamma' L)$  and the algorithmic error dominates. For  $\epsilon \gg \epsilon_c$ , we have  $d \ll k/(\gamma' L)$  and the sampling cost dominates. By combining the above observations with Eq. (55) and Eq. (56), we can obtain the following asymptotic form of  $M(\epsilon)$ :

$$M(\epsilon) \simeq \begin{cases} \frac{1}{\epsilon^2} \left(\frac{\epsilon_c}{\epsilon}\right)^{1/k} \exp\left[2k \left(\frac{\epsilon_c}{\epsilon}\right)^{1/k}\right] & \text{for } \epsilon \ll \epsilon_c, \\ \frac{1}{\epsilon_c^2} e^{2k} & \text{for } \epsilon = \epsilon_c, \\ \frac{1}{\epsilon^2} \left(1 + 2k \left(\frac{\epsilon_c}{\epsilon}\right)^{2/(2k+1)}\right) & \text{for } \epsilon \gg \epsilon_c. \end{cases} \quad (57)$$

Here, we treat  $k = O(1)$  as a constant. In the third case we used the linear approximation  $\exp[2k(\epsilon_c/\epsilon)^{2/(2k+1)}] \simeq 1 + 2k(\epsilon_c/\epsilon)^{2/(2k+1)}$ . This result shows that targeting an accuracy beyond the threshold  $\epsilon_c$  inevitably requires an exponentially large sampling cost. Accordingly, we refer to  $\epsilon_c$  as the *critical error* of the Trotter-based algorithm under PEC. Like the error bound  $\epsilon_b$ , it characterizes a threshold on the attainable accuracy, but unlike a mere bound, the critical error is achievable. Indeed, it is realized by choosing  $d = k/(\gamma' L)$ , which corresponds to sampling overhead  $\Gamma^2 = e^{2k}$ .

Compared to Eq. (40), the critical error exhibits a qualitative improvement, changing from  $O(\alpha_k^{1/(k+1)} (L\gamma)^{k/(k+1)})$  to  $O(\alpha_k (L\gamma)^k)$  (where we use  $\gamma' \propto \gamma$ ), i.e., an improvement in the scaling exponent by a factor of  $k + 1$ .

The exponential barrier in Eq. (57) is inevitable. Indeed, even without considering the statistical error, to

reach a target accuracy  $\epsilon$ , Eq. (17) requires  $d = (\alpha_k/\epsilon)^{1/k}$  Trotter layers. Substituting this scaling into the PEC sampling overhead  $\Gamma = e^{Ld\gamma'}$  gives  $\Gamma = e^{L\gamma'(\alpha_k/\epsilon)^{1/k}} \simeq e^{(\epsilon_c/\epsilon)^{1/k}}$ . Because this exponential overhead dominates at large  $d$ , the same exponential dependence on  $\epsilon$  persists in the full expression Eq. (57) whenever  $\epsilon \ll \epsilon_c$ , which hinders the accuracy improvement beyond the critical error. In contrast, as we will see next, the randomized LCU algorithm has a gate count that is independent of the target accuracy, so the corresponding  $M(\epsilon)$  does not exhibit an exponential dependence on  $\epsilon$ .

Because the qDrift algorithm [27] exhibits a similar scaling as the first-order Trotter formula, namely that the algorithmic error is inversely proportional to the number of algorithmic layers, we can analogously optimize the circuit depth and determine the critical error threshold.

### B. Randomized linear combination of unitaries

We now turn to the randomized LCU algorithm combined with PEC. Unlike the Trotter case, where PEC must compensate for both algorithmic and physical errors, the RLCU estimator is inherently unbiased. Thus, the optimization reduces to minimizing the sampling overhead with respect to the repetition parameter  $r$ . Because the RLCU estimator is unbiased, the end-to-end performance is governed by the sampling overhead, which we aim to optimize with respect to the simulation time  $t$ . Because the circuit depth of RLCU is a random variable determined by the sampled Taylor order  $k$ , the PEC cost must be evaluated after averaging over this depth distribution. The following theorem bounds the expected sampling overhead of RLCU combined with PEC.

**Theorem 2.** *The MSE of this algorithm is bounded by*

$$\epsilon^2 \leq \frac{1}{M} \exp\left(\frac{\tilde{t}^2}{r} + 2\gamma'r + \tilde{t}(e^{2\gamma_c} - 1)\right). \quad (58)$$

Here,  $\gamma'$  denotes the error rate associated with non-Clifford operations, whereas  $\gamma_c$  denotes that for Clifford operations. Typically,  $\gamma_c \ll \gamma$ .

The proof is given in section C. Because  $\gamma_c \ll 1$ , we may approximate  $e^{2\gamma_c} - 1 \simeq 2\gamma_c$ . As in the Trotter case, we express the result in terms of the number of samples  $M(\epsilon)$  required to achieve a target accuracy  $\epsilon$ . Inverting the mean-squared error bound in Eq. (58) under this approximation gives

$$M(\epsilon) = \frac{1}{\epsilon^2} \exp\left(\frac{\tilde{t}^2}{r} + 2\gamma'r + 2\gamma_c\tilde{t}\right). \quad (59)$$

Now we consider the optimization of the repetition number  $r$ . Chakraborty [12] adopted  $r = \tilde{t}^2 = \beta^2 t^2$  so that the sampling overhead due to RLCU  $\Gamma_{\text{RLCU}} = e^{(\beta t)^2/r}$  is constant. With this strategy, the required number of

TABLE I: Summary of noise-limited accuracy thresholds for Hamiltonian simulation algorithms with and without PEC. We use the fact that  $\gamma' \propto \gamma$  to simplify the notation in scaling analysis.

Algorithm	Without PEC Error bound $\epsilon_b$	With PEC Critical error $\epsilon_c$
Suzuki–Trotter	$O\left(\alpha_k^{1/(k+1)}(L\gamma)^{k/(k+1)}\right)$	$O\left(\alpha_k(L\gamma)^k\right)$
Randomized LCU	$O(\gamma(\beta t)^2)$	N/A

samples becomes

$$M(\epsilon) = \frac{1}{\epsilon^2} \exp(1 + 2\gamma'\tilde{t}^2 + 2\gamma_c\tilde{t}). \quad (60)$$

When the term proportional to  $\tilde{t}^2$  dominates, the leading contribution in the exponent is  $O(\gamma(\beta t)^2)$ . We instead optimize  $M(\epsilon, r)$  in Eq. (59) with respect to the repetition number  $r$ . By balancing the terms  $\tilde{t}^2/r$  and  $2\gamma'r$  in the exponent, the optimal choice  $r^* = \frac{\tilde{t}}{2\gamma'}$ . With this choice, the required number of samples reduces to

$$M(\epsilon) = \frac{1}{\epsilon^2} \exp\left(2\sqrt{2\gamma'\tilde{t}} + 2\gamma_c\tilde{t}\right). \quad (61)$$

In this case, the dominant contribution in the exponent is  $O(\sqrt{\gamma'}\beta t)$  when the square-root term dominates. This result demonstrates a square-root improvement in the exponential scaling compared to the unoptimized choice of  $r = \tilde{t}^2$  in Eq. (60). In other words, optimizing the repetition number reduces the dominant contribution in the PEC overhead from  $O(\gamma'(\beta t)^2)$  to  $O(\sqrt{\gamma'}\beta t)$ , yielding a mitigation of the exponential sampling cost. When  $\sqrt{2\gamma'\tilde{t}} < 1$ , however, the choice  $r = \tilde{t}^2$  already produces a shallower circuit than  $r^*$ , and the PEC overhead no longer dominates the error contribution. In this regime,  $r = \tilde{t}^2$  is therefore preferable in practice. We will come back to this point in section VC1.

Before closing this part, we highlight the key difference between the Trotter-based and RLCU-based algorithms with respect to the accuracy threshold. Importantly, the exponent in Eq. (59) is independent of the target accuracy  $\epsilon$ , which means that, unlike the Trotter-based algorithm, the sampling overhead scales only polynomially with respect to  $\epsilon$ . The error bounds and critical errors for all four cases are summarized in table I. The *error bound*  $\epsilon_b$  is the irreducible MSE floor in the absence of PEC, attained in the limit  $M \rightarrow \infty$ . The *critical error*  $\epsilon_c$  is an analogous threshold under PEC that is achievable at finite cost, while targeting  $\epsilon \ll \epsilon_c$  incurs an exponentially large sampling overhead. For the randomized LCU algorithm combined with PEC, the sampling cost  $M(\epsilon)$  grows only polynomially in  $1/\epsilon$ , so no exponential barrier arises and the concept of a critical error does not apply.

### C. The overhead of characterizing the error

The analysis above assumes perfect knowledge of the noise model. In practice, implementing PEC requires an explicit estimate of the noise parameters, which introduces an additional sampling cost. Here, we assume that we characterize the elementary gate operations, e.g., universal gate set, and the elementary gate errors are static across the entire quantum circuit for simplicity. Let  $\mathcal{N}_k$  denote a noise channel associated with the  $k$ th gate, and let  $\mathcal{N}'_k$  be its estimated inverse noise channel obtained from gate set tomography (GST) [20, 31, 32]. Then, we write the maximum estimation error as

$$\Delta\gamma := \max_k D(\mathcal{N}'_k \circ \mathcal{N}_k, \mathcal{I}), \quad (62)$$

and assume the standard scaling with respect to the number of GST samples  $M_g$ ,

$$\Delta\gamma = O\left(\frac{1}{\sqrt{M_g}}\right), \quad (63)$$

up to constants that depend on the particular GST protocol and the underlying noise.

*Bias induced by characterization errors* – When PEC is constructed using  $\hat{\gamma}_k$  instead of the true  $\gamma_k$ , the resulting estimator  $\hat{\mu}$  for an observable expectation value generally becomes biased. A simple bound is obtained by summing the worst-case contribution of each gate:

$$|\text{Bias}(\hat{\mu})| \leq O(N_g/\sqrt{M_g}), \quad (64)$$

where  $N_g$  is the number of elementary gates in the executed circuit (corresponding to  $N_G$  in the general PEC formalism of section IV). See Appendix E for the derivation. For the RLCU algorithm, as we discussed in section III B, the estimator is further reweighted by the sampling overhead  $\Gamma_{\text{RLCU}}$ , and the corresponding bias bound becomes  $\Gamma_{\text{RLCU}} N_g \Delta\gamma$ . Using the GST scaling (63), this translates into a sufficient number of GST samples

$$M_g = O\left(\frac{N_g^2}{\epsilon^2}\right), \quad (65)$$

where  $\epsilon$  is the target accuracy for the observable expectation value. For the randomized LCU algorithm, the sampling cost scales as

$$M_g = O\left(\frac{\Gamma_{\text{RLCU}}^2 N_g^2}{\epsilon^2}\right), \quad (66)$$

To assess the relative weight of this overhead, we define the simulation cost  $\mathcal{R} := dLM$  (for Suzuki–Trotter) or  $\mathcal{R} := rM$  (for RLCU) as the product of the depth parameter per circuit and the number of circuit samples  $M$ , which characterize the coarse simulation time for the Hamiltonian simulation. Then, the ratio  $M_g/\mathcal{R}$  quantifies whether the characterization cost is a significant fraction of the total simulation budget. We now evaluate this ratio for both the Suzuki–Trotter and randomized LCU algorithms.

#### 1. Suzuki–Trotter and GST Cost

We first benchmark the characterization overhead against the conventional Suzuki–Trotter approach in two regimes of the target precision in Eq. (57). Fixing a target mean-squared error  $\epsilon^2$ , we can express the optimal number of Trotter layers  $d^*$  and the required number of circuit samples  $M$  as functions of  $\epsilon$ . In the regime  $\epsilon \ll \epsilon_c$ , from Eq. (56) and Eq. (57), we have

$$d^* \simeq \frac{k}{\gamma' L} \left(\frac{\epsilon_c}{\epsilon}\right)^{1/k}, \quad (67)$$

$$M \simeq \frac{1}{\epsilon^2} \left(\frac{\epsilon_c}{\epsilon}\right)^{1/k} \exp\left[2k \left(\frac{\epsilon_c}{\epsilon}\right)^{1/k}\right], \quad (68)$$

and in the regime  $\epsilon \gg \epsilon_c$ , we have

$$d^* \simeq \frac{k}{\gamma' L} \left(\frac{\epsilon_c}{\epsilon}\right)^{2/(2k+1)}, \quad (69)$$

$$M = \frac{1}{\epsilon^2} \left(1 + 2k \left(\frac{\epsilon_c}{\epsilon}\right)^{2/(2k+1)}\right). \quad (70)$$

By noting that the number of elementary gates is  $N_g = d^*L$ , we obtain the GST sampling cost to achieve the target accuracy  $\epsilon$  as

$$M_g = \begin{cases} O\left(\left[\frac{k}{\gamma'\epsilon} \left(\frac{\epsilon_c}{\epsilon}\right)^{1/k}\right]^2\right) & \epsilon \ll \epsilon_c, \\ O\left(\left(\frac{k}{\gamma'\epsilon_c}\right)^2\right) & \epsilon = \epsilon_c, \\ O\left(\left[\frac{k}{\gamma'\epsilon} \left(\frac{\epsilon_c}{\epsilon}\right)^{2/(2k+1)}\right]^2\right) & \epsilon \gg \epsilon_c, \end{cases} \quad (71)$$

and by using  $\mathcal{R} = d^*LM$ , the ratio between the GST sampling cost and the simulation cost scales as

$$\frac{M_g}{\mathcal{R}} = \begin{cases} O\left(\frac{k}{\gamma'} \exp\left[-2k \left(\frac{\epsilon_c}{\epsilon}\right)^{1/k}\right]\right) & \epsilon \ll \epsilon_c, \\ O\left(\frac{k}{\gamma'} e^{-2k}\right) & \epsilon = \epsilon_c, \\ O\left(\frac{k}{\gamma'} \left(\frac{\epsilon_c}{\epsilon}\right)^{2/(2k+1)} \left(1 + 2k \left(\frac{\epsilon_c}{\epsilon}\right)^{2/(2k+1)}\right)^{-1}\right) & \epsilon \gg \epsilon_c. \end{cases} \quad (72)$$

In the regime  $\epsilon \ll \epsilon_c$ , the exponential factor suppresses the ratio, so that the GST cost is negligible compared to the Hamiltonian-simulation cost because the PEC sampling overhead dominates the total budget. In the regime  $\epsilon \gg \epsilon_c$ , the ratio scales as  $O(k/\gamma')$  up to a polynomial correction in  $\epsilon_c/\epsilon$ . This indicates that the characterization cost becomes more significant as the per-gate error  $\gamma$  decreases.

#### 2. Randomized LCU

For randomized LCU, following a similar argument as for Eq. (45), the expected gate count per circuit is  $N_g =$

$r + (\beta t)^2/r$ . As discussed in Eq. (59), the choice of the repetition number depends on whether  $\sqrt{2\gamma'}\beta t$  exceeds 1. In the regime  $\sqrt{2\gamma'}\beta t \geq 1$ , we use the optimized value  $r^* = \beta t/\sqrt{2\gamma'}$ , which offers a smaller sampling cost and shallower circuit depth than the choice of  $r = (\beta t)^2$ , while in the regime  $\sqrt{2\gamma'}\beta t \leq 1$ , we set  $r = (\beta t)^2$ . In both cases, the second term is negligible compared to the first so we can safely approximate  $N_g \simeq r$ . Using Eq. (66), the GST sampling cost to achieve the target accuracy  $\epsilon$  is

$$M_g = \begin{cases} O\left(\Gamma_{\text{RLCU}}^2 \frac{(\beta t)^2}{2\gamma' \epsilon^2}\right) & \sqrt{2\gamma'}\beta t \geq 1, \\ O\left(\frac{(\beta t)^4}{\epsilon^2}\right) & \sqrt{2\gamma'}\beta t \leq 1. \end{cases} \quad (73)$$

Here, to obtain the upper bound for  $\sqrt{2\gamma'}\beta t \geq 1$ , we select  $r^* = (\beta t)^2$  so that  $\Gamma_{\text{RLCU}} \leq \exp((\beta t)^2/r^*) = e = O(1)$ .

As in the Suzuki–Trotter case, we compare the characterization cost  $M_g$  with the overall simulation cost  $\mathcal{R} = r^*M$ . Then, the ratio between the GST sampling cost and the simulation cost scales as

$$\frac{M_g}{\mathcal{R}} = \begin{cases} O\left(\frac{\beta t}{\sqrt{2\gamma'}}\right) & \sqrt{2\gamma'}\beta t \geq 1, \\ O((\beta t)^2) & \sqrt{2\gamma'}\beta t \leq 1. \end{cases} \quad (74)$$

Note that  $\Gamma_{\text{RLCU}}$  is cancelled out in the ratio in the first regime.

Importantly, in both the Suzuki–Trotter and randomized LCU cases, the resource ratio  $M_g/\mathcal{R}$  scales as  $O(1/\gamma')$  as  $\gamma'$  decreases (i.e., as gate fidelity improves). This can be understood intuitively as follows. Suppose the per-gate error rate is  $\gamma$ . To remove the noise-induced bias via PEC, the noise model must be determined to a precision higher than  $\gamma$  itself; otherwise, the residual characterization error would dominate the mitigated result. Consequently, the sampling cost required for noise-model characterization scales inversely with  $\gamma$ , explaining the observed growth of  $M_g/\mathcal{R}$  in the high-fidelity regime.

## VI. ERROR-MITIGATED HAMILTONIAN SIMULATION WITH THE SPACE-TIME NOISE INVERSION METHOD

In the previous section, the characterization cost of standard PEC via standard GST can become significant, particularly as the per-gate error decreases (Eq. (72)). To improve this scaling, we now consider the space-time noise inversion (SNI) method [28], a recently proposed PEC variant that characterizes only the aggregate error probability of the entire circuit rather than individual gate errors. This method is particularly suited to the early FTQC era, where high-fidelity logical qubits are available but qubit resources are scarce.

### A. Space-time noise inversion

The space-time noise inversion (SNI) method aims to invert the noise across the entire quantum circuit by treating it as a single space-time noise model. More specifically, when the noisy quantum process in the quantum circuit is described as  $\prod_{k=1}^{N_G} \mathcal{N}_k \mathcal{U}_k$ , the space-time noise is described as  $\mathcal{N}_{\text{ST}} = \mathcal{N}_{N_G} \otimes \mathcal{N}_{N_G-1} \otimes \cdots \otimes \mathcal{N}_1$ . This method assumes that the noise model is described by stochastic Pauli noise via twirling techniques. Then, the space-time noise is represented as  $\mathcal{N}_{\text{ST}} = (1 - p_{\text{ST}})\mathcal{I} + p_{\text{ST}}\mathcal{E}$ , where  $\mathcal{E}$  corresponds to the process for Pauli-error events and  $p_{\text{ST}}$  is the total error probability of the circuit. Then, SNI inverts the entire space-time noise as

$$\mathcal{N}_{\text{ST}}^{-1} = \sum_{l=0}^{\infty} \frac{(-1)^l p_{\text{ST}}^l}{(1 - p_{\text{ST}})^{l+1}} \mathcal{E}^l \quad (75)$$

for  $p_{\text{ST}} < 1/2$ . The cost for this quasi-probability decomposition is  $\Gamma = \sum_{l=0}^{\infty} p_{\text{ST}}^l / (1 - p_{\text{ST}})^{l+1} = 1/(1 - 2p_{\text{ST}})$ . To perform Eq. (75), (i) we only need to know the single error probability  $p_{\text{ST}}$  and (ii) sample  $\mathcal{E}^l$ . To do so, we use a quantum circuit that performs Bell measurements for each noisy quantum operation  $\mathcal{N}_k \mathcal{U}_k$  using twice the number of logical qubits. Crucially, while the sampling is performed at the gadget level, these samples are aggregated to characterize the single global error probability  $p_{\text{ST}}$ . The sampling cost for characterizing the error probability  $p_{\text{ST}}$  scales as  $M_{p_{\text{ST}}} = O(\epsilon^{-2}(1 - 2p_{\text{ST}})^{-4})$ , with the required number of circuit runs for the computation circuit being  $M = O(\epsilon^{-2}(1 - 2p_{\text{ST}})^{-2})$  to certify the total computation accuracy of the error-mitigated computation to  $\epsilon$ . Note that the SNI method is also compatible with the randomized compiling, mid-circuit measurement, and feedback operations; therefore, SNI is compatible with the randomized LCU algorithm as well. While the SNI sampling cost is divergent at  $p_{\text{ST}} = 1/2$ , this problem can be circumvented by separating the quantum circuit into  $R$  segments. By applying SNI to each segment individually where the local error rate is well below  $1/2$ , the total sampling cost is determined by the product of the costs for each segment, thus avoiding the singularity.

### B. Improved characterization scaling via space-time noise inversion

We now consider applying PEC via the space-time noise inversion method to the Hamiltonian simulation algorithms discussed above. Let us assume that the total error probability of the entire quantum circuit is given by  $p_{\text{ST}}$ . Using the worst-case per-gate error rate  $\gamma$  introduced in Eq. (37), the total space-time error probability for a circuit consisting of  $dL$ -gates is bounded by  $p_{\text{ST}} = 1 - (1 - \gamma)^{dL} \simeq 1 - e^{-\gamma dL}$ . If  $p_{\text{ST}} < 1/2$ , the SNI method can be applied directly to the entire circuit.

However, when  $p_{\text{ST}} \geq 1/2$ , the SNI sampling cost diverges, and it becomes necessary to partition the circuit into  $s$  segments, as discussed in the previous subsection. Because both the Suzuki–Trotter formula and the RLCU algorithm consist of repeated applications of an identical circuit structure, we assume that the total error probability is uniform across all segments. Let  $q = 1 - (1 - \gamma)^L$  denote the upper bound of the per-layer error probability. Note also that  $q \leq \gamma L$ . Under this assumption, let  $q_{\text{ST}}$  denote the space-time error probability per segment, given by

$$q_{\text{ST}} = 1 - (1 - q)^{d/s}. \quad (76)$$

In this segmented implementation, the sampling cost required to characterize the error probability  $q_{\text{ST}}$  scales as

$$M_{q_{\text{ST}}} = O\left(\epsilon^{-2} s^2 (1 - 2q_{\text{ST}})^{-4}\right), \quad (77)$$

while the number of circuit executions required for the error-mitigated computation scales as

$$M = O\left(\epsilon^{-2} (1 - 2q_{\text{ST}})^{-2s}\right). \quad (78)$$

At first glance, Eq. (78) may appear to differ from the PEC overhead scaling in Eq. (53). However, the following inequality shows that it can be written in a closely related form:

$$\exp(4qd) < (1 - 2q_{\text{ST}})^{-2s} < \exp\left(\frac{4qd}{1 - 2qd/s}\right). \quad (79)$$

We detail the derivation of bound in section D. If we choose the number of segments  $s$  so that  $1 - 2qd/s = c$  for a positive constant  $c$ , the upper bound becomes  $M = O(\epsilon^{-2} \exp(4qd/c))$ . Because this has the same functional form as Eq. (54), the optimization of the layer count  $d$  follows the same argument that leads to Eq. (57), with  $L\gamma'$  replaced by  $2q/c \leq 2L\gamma/c$ . Furthermore, if we choose  $s = 4qd$ , corresponding to  $c = 1/2$ , the scalings are roughly

$$\begin{aligned} M_{q_{\text{ST}}} &= O\left(\epsilon^{-2} (Ld\gamma)^2\right), \\ M &= O\left(\epsilon^{-2} \exp(8Ld\gamma)\right). \end{aligned} \quad (80)$$

Here we used  $q_{\text{ST}} \leq qd/s$  and  $q \leq \gamma L$ . In the practical regime where  $Ld\gamma = O(1)$ , the characterization cost no longer increases as  $\gamma \rightarrow 0$  while keeping  $Ld\gamma = O(1)$ , unlike the naive GST approach where  $M_g$  scales as  $O(\gamma^{-1})$  as  $\gamma \rightarrow 0$ .

To quantify the resource ratio between the characterization and simulation costs, we evaluate the ratio  $M_{q_{\text{ST}}}/\mathcal{R}$  with  $\mathcal{R} = dLM$ . Substituting  $M_{q_{\text{ST}}} = O(\epsilon^{-2}(qd)^2)$  and  $M = O(\epsilon^{-2} \exp(4qd))$  yields

$$\frac{M_{q_{\text{ST}}}}{\mathcal{R}} = O\left(\frac{q^2 d}{L e^{4qd}}\right) = O(\gamma \cdot qd e^{-4qd}), \quad (81)$$

where we used  $q^2/L \leq \gamma q$  from  $q \leq \gamma L$ . Because  $x e^{-4x} \leq 1/(4e)$  for all  $x \geq 0$ , the noise-characterization cost is

exponentially smaller than the simulation cost whenever  $qd \gg 1$ . Even in the worst case,  $M_{q_{\text{ST}}}/\mathcal{R} = O(1)$ .

SNI avoids the divergence of the sampling cost for a small error rate observed in GST by characterizing only the aggregate error probability  $q_{\text{ST}}$  per segment rather than the full per-gate noise model, resulting in a characterization cost that is smaller or comparable to the Hamiltonian simulation cost. Note that the same analysis applies to the randomized LCU algorithm by replacing  $dL$  with  $r$  and noting that  $N_g \simeq r$  (see Eq. (45)). Specifically, the characterization and simulation costs become  $M_{q_{\text{ST}}} = O(\epsilon^{-2} \Gamma_{\text{RLCU}}^2 (r\gamma)^2)$  and  $M = O(\epsilon^{-2} \Gamma_{\text{RLCU}}^2 \exp(8r\gamma))$ , respectively. With  $\mathcal{R} = rM$ , the ratio satisfies  $M_{q_{\text{ST}}}/\mathcal{R} = O(1)$  by the same argument as in the Trotter case. Because the segmented SNI overhead retains the same functional form  $\exp(O(\gamma N_g))$  regardless of the underlying algorithm, SNI can be used to efficiently characterize the noise model for a wide range of Hamiltonian simulation algorithms.

## VII. CONCLUSIONS AND DISCUSSIONS

In this work, we propose optimizing the number of layers in Hamiltonian simulation algorithms, i.e., Trotter and LCU-based algorithms, to minimize the mean-squared error (MSE) that accounts for both physical and algorithmic contributions. For the Trotter-based simulation, we show that the sampling cost exhibits two distinct regimes as a function of the target accuracy: a polynomial regime and an exponential regime. This implies the existence of a critical error  $\epsilon_c$ , beyond which further accuracy improvements require an exponentially growing number of samples. For the randomized LCU-based algorithm, we can realize an unbiased estimator of the target observable via the single-ancilla LCU construction. Moreover, the circuit depth is a random variable with a bounded expectation, and the additional depth required to improve the simulation accuracy is practically negligible, so that the end-to-end performance is governed primarily by sampling overhead rather than a systematic algorithmic bias.

Building on this, we optimize the repetition number  $r$ . By balancing the terms  $\tilde{t}^2/r$  and  $2\gamma'r$  in the exponent of the MSE bound, we obtain an optimal choice  $r^* = \tilde{t}/\sqrt{2\gamma'}$ , which yields a square-root improvement in the dominant time dependence of the exponential sampling cost, from  $O(\gamma(\beta t)^2)$  for example when  $r = \tilde{t}^2$  to  $O(\sqrt{\gamma} \beta t)$ . In addition, we quantify the sampling overhead associated with gate set tomography (GST) required for error mitigation, and we further evaluate how space-time noise inversion (SNI) can improve the scaling of this overhead.

Note that our approach can be naturally extended to other types of Hamiltonian simulation algorithms. In particular, the recently proposed TE-PAI method [33] enables the computation of unbiased estimators of expectation values via random sampling of a quantum cir-

cuit, based on the quasi-probability decomposition of the Trotter algorithm with the probabilistic angle interpolation [34]. Because the sample complexity of this method can be controlled at the cost of the depth of the circuit (denoted as the  $Q$  parameter in Ref. [33]), similarly to the parameter  $r$  in the randomized LCU, there is room to optimize the depth when combined with the QEM.

Furthermore, while we focus on the PEC method, it is worth investigating other QEM methods for Hamiltonian simulation. For example, the virtual distillation [35, 36] and the extrapolation [15, 19] do not require the explicit information of noise, so they may reduce the total complexity of error-mitigated Hamiltonian simulation. Furthermore, the unification of QEM methods, via e.g., generalized quantum subspace expansion [37, 38], may further reduce both physical and algorithmic errors. In addition, integrating and balancing our approach with algorithmic QEM methods [14, 39] may be valuable for achieving efficient near-term Hamiltonian simulation.

Finally, the optimization of algorithmic resources for minimizing QEM sampling overhead is likely relevant beyond real-time Hamiltonian simulation. Similar optimization principles may apply to a broad range of

quantum algorithms, such as quantum linear system solvers [10, 11, 40], ground-state estimation [41, 42], and density-matrix exponentiation [43, 44]. In addition, recent studies of quantum-classical hybrid implementations of linear-combination-of-unitaries methods indicate that quantum resources, including circuit depth and ancilla usage, can be traded against classical sampling overhead [45]. It would therefore be important to extend such resource-trade-off analyses by explicitly incorporating the cost of quantum error mitigation and identifying the optimal quantum-classical balance under noise.

## ACKNOWLEDGMENTS

This work was supported by JSPS KAKENHI Grant Numbers 24KJ0892, 20H01824 and 24K00543, the Center of Innovation for Sustainable Quantum AI (SQAI), and JST Grant Number JPMJPF2221; JST [Moonshot R&D] Grant No. JPMJMS2061; MEXT Q-LEAP, Grant No. JPMXS0120319794 and No. JPMXS0118067285; and JST CREST Grant No. JPMJCR23I4 and No. JPMJCR25I4.

- 
- [1] S. Lloyd, *Science* **273**, 1073 (1996).
  - [2] D. W. Berry, A. M. Childs, R. Cleve, R. Kothari, and R. D. Somma, *Physical review letters* **114**, 090502 (2015).
  - [3] G. H. Low and I. L. Chuang, *Quantum* **3**, 163 (2019).
  - [4] A. Y. Kitaev, arXiv preprint quant-ph/9511026 (1995).
  - [5] A. Aspuru-Guzik, A. D. Dutoi, P. J. Love, and M. Head-Gordon, *Science* **309**, 1704 (2005).
  - [6] L. Lin and Y. Tong, *PRX quantum* **3**, 010318 (2022).
  - [7] K. Wan, M. Berta, and E. T. Campbell, *Physical Review Letters* **129**, 030503 (2022).
  - [8] D. An, J.-P. Liu, and L. Lin, *Physical Review Letters* **131**, 150603 (2023).
  - [9] D. An, A. M. Childs, and L. Lin, *Communications in Mathematical Physics* **407**, 19 (2026).
  - [10] A. M. Childs, R. Kothari, and R. D. Somma, *SIAM Journal on Computing* **46**, 1920 (2017).
  - [11] S. Wang, S. McArdle, and M. Berta, *PRX quantum* **5**, 020324 (2024).
  - [12] S. Chakraborty, *Quantum* **8**, 1496 (2024).
  - [13] G. C. Knee and W. J. Munro, *Physical Review A* **91**, 052327 (2015).
  - [14] S. Endo, Q. Zhao, Y. Li, S. Benjamin, and X. Yuan, *Physical Review A* **99**, 012334 (2019).
  - [15] P. Mohammadipour and X. Li, *Quantum* **9**, 1909 (2025).
  - [16] S. Hakkaku, Y. Suzuki, Y. Tokunaga, and S. Endo, arXiv preprint arXiv:2503.05052 (2025).
  - [17] J. Xu, C. Zhao, J. Fan, and Q. Zhao, arXiv preprint arXiv:2504.10247 (2025).
  - [18] Y. Li and S. C. Benjamin, *Physical Review X* **7**, 021050 (2017).
  - [19] K. Temme, S. Bravyi, and J. M. Gambetta, *Physical review letters* **119**, 180509 (2017).
  - [20] S. Endo, S. C. Benjamin, and Y. Li, *Physical Review X* **8**, 031027 (2018).
  - [21] Z. Cai, R. Babbush, S. C. Benjamin, S. Endo, W. J. Huggins, Y. Li, J. R. McClean, and T. E. O’Brien, *Reviews of Modern Physics* **95**, 045005 (2023).
  - [22] S. Endo, Z. Cai, S. C. Benjamin, and X. Yuan, *Journal of the Physical Society of Japan* **90**, 032001 (2021).
  - [23] D. Aharonov, O. Alberton, I. Arad, Y. Atia, E. Bairey, Z. Brakerski, I. Cohen, O. Golan, I. Gurwich, O. Keneth, *et al.*, arXiv preprint arXiv:2503.17243 (2025).
  - [24] Z. Cai, arXiv preprint arXiv:2110.05389 (2021).
  - [25] D. W. Berry, G. Ahokas, R. Cleve, and B. C. Sanders, *Communications in Mathematical Physics* **270**, 359 (2007).
  - [26] A. M. Childs, Y. Su, M. C. Tran, N. Wiebe, and S. Zhu, *Phys. Rev. X* **11**, 011020 (2021).
  - [27] E. Campbell, *Phys. Rev. Lett.* **123**, 070503 (2019).
  - [28] H. Xie, N. Yoshioka, K. Tsubouchi, and Y. Li, *Physical Review Letters* **136**, 010603 (2026).
  - [29] B. Regula, R. Takagi, and M. Gu, *Quantum* **5**, 522 (2021).
  - [30] J. Jiang, K. Wang, and X. Wang, *Quantum* **5**, 600 (2021).
  - [31] E. Nielsen, J. K. Gamble, K. Rudinger, T. Scholten, K. Young, and R. Blume-Kohout, *Quantum* **5**, 557 (2021).
  - [32] D. Greenbaum, arXiv preprint arXiv:1509.02921 (2015).
  - [33] C. Kiumi and B. Koczor, *Quantum Science and Technology* **10**, 045071 (2025).
  - [34] B. Koczor, J. J. Morton, and S. C. Benjamin, *Physical Review Letters* **132**, 130602 (2024).
  - [35] W. J. Huggins, S. McArdle, T. E. O’Brien, J. Lee, N. C. Rubin, S. Boixo, K. B. Whaley, R. Babbush, and J. R. McClean, *Physical Review X* **11**, 041036 (2021).
  - [36] B. Koczor, *Physical Review X* **11**, 031057 (2021).

- [37] N. Yoshioka, H. Hakoshima, Y. Matsuzaki, Y. Tokunaga, Y. Suzuki, and S. Endo, *Physical Review Letters* **129**, 020502 (2022).
- [38] B. Yang, N. Yoshioka, H. Harada, S. Hakkaku, Y. Tokunaga, H. Hakoshima, K. Yamamoto, and S. Endo, *Physical Review Applied* **23**, 054021 (2025).
- [39] J. D. Watson and J. Watkins, *PRX Quantum* **6**, 030325 (2025).
- [40] A. W. Harrow, A. Hassidim, and S. Lloyd, *Physical review letters* **103**, 150502 (2009).
- [41] Y. Ge, J. Tura, and J. I. Cirac, *Journal of Mathematical Physics* **60** (2019).
- [42] P. Zeng, J. Sun, and X. Yuan, arXiv preprint arXiv:2109.15304 (2021).
- [43] S. Lloyd, M. Mohseni, and P. Rebentrost, *Nature physics* **10**, 631 (2014).
- [44] K. Wada, J. Kato, H. Harada, and N. Yamamoto, arXiv preprint arXiv:2509.14791 (2025).
- [45] K. Wada, H. Harada, Y. Suzuki, Y. Tokunaga, N. Yamamoto, and S. Endo, arXiv preprint arXiv:2512.06260 (2025).

### Appendix A: Unified measure of estimation quality: mean-squared error (MSE)

In this appendix, we review the basic properties of the mean-squared error (MSE) and explain why it is a useful unified measure of estimation quality. For an estimator  $\hat{\theta}$  of a parameter  $\theta$ , there are two main sources of error. First, the estimator may suffer from a *systematic error* (bias), defined by

$$\text{Bias}(\hat{\theta}) = \mathbb{E}[\hat{\theta}] - \theta. \quad (\text{A1})$$

Bias measures the extent to which the estimator is centered away from the true value, and therefore quantifies lack of accuracy due to systematic deviation. Second, the estimator is subject to *sampling variability*, measured by its variance,

$$\text{Var}(\hat{\theta}) = \mathbb{E}[(\hat{\theta} - \mathbb{E}[\hat{\theta}])^2]. \quad (\text{A2})$$

Variance quantifies the dispersion of repeated estimates around their own mean, and therefore reflects statistical precision. The mean-squared error combines these two contributions into a single measure:

$$\text{MSE}(\hat{\theta}) = \mathbb{E}[(\hat{\theta} - \theta)^2]. \quad (\text{A3})$$

Expanding around  $\mathbb{E}[\hat{\theta}]$  gives

$$\text{MSE}(\hat{\theta}) = \mathbb{E}[(\hat{\theta} - \mathbb{E}[\hat{\theta}] + \mathbb{E}[\hat{\theta}] - \theta)^2] \quad (\text{A4})$$

$$= \mathbb{E}[(\hat{\theta} - \mathbb{E}[\hat{\theta}])^2] + (\mathbb{E}[\hat{\theta}] - \theta)^2 \quad (\text{A5})$$

$$= \text{Var}(\hat{\theta}) + \text{Bias}(\hat{\theta})^2. \quad (\text{A6})$$

This decomposition shows that MSE accounts for both random fluctuations and systematic deviation. For this reason, MSE is a natural measure of *overall estimation error*. In particular, variance alone measures precision, whereas MSE evaluates estimator quality when both precision and accuracy are relevant. An estimator with small variance but large bias may still have poor overall performance, and MSE captures this trade-off directly. Therefore, when both sampling error and systematic error are present, it is statistically correct to use MSE as a unified criterion for comparing estimators or for quantifying overall uncertainty.

Since  $\mathbb{E}[(\hat{\theta} - \theta)^2] = \text{MSE}(\hat{\theta})$ , the Chebyshev inequality gives

$$\Pr(|\hat{\theta} - \theta| \geq a) \leq \frac{\text{MSE}(\hat{\theta})}{a^2}. \quad (\text{A7})$$

Taking the complement,

$$\Pr(|\hat{\theta} - \theta| < a) \geq 1 - \frac{\text{MSE}(\hat{\theta})}{a^2}. \quad (\text{A8})$$

To guarantee at least  $1 - \alpha$  coverage, set

$$a = \sqrt{\frac{\text{MSE}(\hat{\theta})}{\alpha}}, \quad (\text{A9})$$

which yields

$$\Pr\left(\theta \in \hat{\theta} \pm \sqrt{\frac{\text{MSE}(\hat{\theta})}{\alpha}}\right) \geq 1 - \alpha. \quad (\text{A10})$$

Thus an MSE-based confidence bound is valid in this distribution-free, conservative sense:

$$\theta \in \hat{\theta} \pm \sqrt{\frac{\text{MSE}(\hat{\theta})}{\alpha}}. \quad (\text{A11})$$

### Appendix B: Proof of Theorem 1

*Proof.* The mean value of  $k$  is

$$\mathbb{E}_p[k] = \sum_{k \in \text{even}} k p(k, \lambda), \quad (\text{B1})$$

where

$$p(k, \lambda) = \begin{cases} \frac{\frac{\lambda^k}{k!} \sqrt{1 + \left(\frac{\lambda}{k+1}\right)^2}}{\sum_{k' \in \text{even}} \frac{\lambda^{k'}}{k'!} \sqrt{1 + \left(\frac{\lambda}{k'+1}\right)^2}} & k \text{ even,} \\ 0 & k \text{ odd.} \end{cases} \quad (\text{B2})$$

Define the decreasing weight

$$a_k := \sqrt{1 + \left(\frac{\lambda}{k+1}\right)^2}, \quad (\text{B3})$$

and the even-Poisson reference distribution

$$q(k, \lambda) := \begin{cases} \frac{\lambda^k/k!}{\sum_{k' \in \text{even}} \lambda^{k'}/k'!} = \frac{\lambda^k/k!}{\cosh \lambda}, & k \text{ even,} \\ 0, & k \text{ odd.} \end{cases} \quad (\text{B4})$$

Then  $p$  can be written as

$$p(k, \lambda) = \frac{q(k, \lambda) a_k}{\sum_{j \in \text{even}} q(j, \lambda) a_j}. \quad (\text{B5})$$

Because  $a_k$  is decreasing in  $k$ , for any increasing function  $f(k)$  we have

$$\mathbb{E}_p[f(k)] = \frac{\sum_k q(k, \lambda) f(k) a_k}{\sum_k q(k, \lambda) a_k} \leq \sum_k q(k, \lambda) f(k) = \mathbb{E}_q[f(k)]. \quad (\text{B6})$$

Applying this to  $f(k) = k$  and  $f(k) = k^2$  gives

$$\mathbb{E}_p[k] \leq \mathbb{E}_q[k], \quad \mathbb{E}_p[k^2] \leq \mathbb{E}_q[k^2]. \quad (\text{B7})$$

It remains to compute the moments under  $q$ . Using the moment generating function

$$M_q(t) = \sum_k q(k, \lambda) e^{tk} = \frac{\cosh(\lambda e^t)}{\cosh \lambda}, \quad (\text{B8})$$

we obtain

$$\begin{aligned} \mathbb{E}_q[k] &= M'_q(0) = \lambda \tanh \lambda, \\ \mathbb{E}_q[k^2] &= M''_q(0) = \lambda(\lambda + \tanh \lambda) = \lambda^2 + \lambda \tanh \lambda, \end{aligned} \quad (\text{B9})$$

which proves (33)–(34). □

### Appendix C: Proof of Theorem 2

*Proof.* Under PEC the estimator is unbiased for the ideal expectation value, hence the MSE reduces to the variance. Consider one shot of RLCU with PEC. Let  $\hat{\nu}$  be the measured outcome of the bounded observable in that shot, so that  $|\hat{\nu}| \leq 1$ . The shot is reweighted by the RLCU sampling overhead and the PEC overhead, so the single-shot random variable can be written as

$$Z = \Gamma_{\text{RLCU}} \Gamma_{\text{PEC}}(\omega) \hat{\nu}, \quad (\text{C1})$$

where  $\omega$  denotes the randomness in the sampled LCU terms and in PEC. With  $M$  independent shots,  $\hat{\mu} = \frac{1}{M} \sum_{j=1}^M Z_j$ , and therefore

$$\epsilon^2 = \frac{1}{M} \text{Var}(Z) \leq \frac{1}{M} \mathbb{E}[Z^2] \leq \frac{\Gamma_{\text{RLCU}}^2}{M} \mathbb{E}[\Gamma_{\text{PEC}}(\omega)^2], \quad (\text{C2})$$

using  $\text{Var}(Z) \leq \mathbb{E}[Z^2]$  and  $|\hat{\nu}| \leq 1$ . For RLCU we use the standard bound

$$\Gamma_{\text{RLCU}}^2 \leq \exp\left(\frac{\tilde{t}^2}{r}\right). \quad (\text{C3})$$

It remains to bound  $\mathbb{E}[\Gamma_{\text{PEC}}(\omega)^2]$ . For a given realization, the Taylor order in segment  $j$  is an even integer  $k_j$  sampled from  $p(k, \lambda)$  with  $\lambda = \tilde{t}/r$ . In our gate model, the number of elementary operations in that segment is at most  $(1 + k_j)$ , hence the total gate count satisfies

$$N_g(\omega) \leq \sum_{j=1}^r (1 + k_j) = \left( r + \sum_{j=1}^r k_j \right). \quad (\text{C4})$$

Here, the first term corresponds to the number of non-Clifford gates, and the second term to the number of Clifford gates. We can express the PEC cost by using this value as

$$\Gamma_{\text{PEC}}(\omega)^2 \leq \exp\left( 2\gamma' r + 2\gamma_c \sum_{j=1}^r k_j \right), \quad (\text{C5})$$

where we have assigned the per-segment non-Clifford contribution to  $\gamma'$  and the  $k_j$  Clifford contributions to  $\gamma_c$ . Therefore,

$$\begin{aligned} \mathbb{E}[\Gamma_{\text{PEC}}(\omega)^2] &\leq \mathbb{E}\left[ \exp\left( 2\gamma' r + 2\gamma_c \sum_{j=1}^r k_j \right) \right] \\ &= \exp(2\gamma' r) \left( \mathbb{E}_p[e^{2\gamma_c k}] \right)^r, \end{aligned} \quad (\text{C6})$$

because the  $k_j$  are i.i.d.

To bound  $\mathbb{E}_p[e^{2\gamma_c k}]$ , we use the same argument as in Lemma 1. Write  $p(k, \lambda) \propto q(k, \lambda) a_k$  where  $q(k, \lambda)$  is the even-Poisson reference distribution and  $a_k = \sqrt{1 + (\lambda/(k+1))^2}$  is decreasing in  $k$ . Because  $e^{2\gamma_c k}$  is increasing in  $k$ , this implies

$$\mathbb{E}_p[e^{2\gamma_c k}] \leq \mathbb{E}_q[e^{2\gamma_c k}]. \quad (\text{C7})$$

From Eq. (B8), we have

$$\mathbb{E}_q[e^{2\gamma_c k}] = \frac{\cosh(\lambda e^{2\gamma_c})}{\cosh(\lambda)} \leq e^{\lambda(e^{2\gamma_c} - 1)}, \quad (\text{C8})$$

Therefore,

$$\mathbb{E}_q[e^{2\gamma_c k}] \leq \exp(\lambda(e^{2\gamma_c} - 1)), \quad (\text{C9})$$

Plugging this into the previous bound and using  $r\lambda = \tilde{t}$  gives

$$\mathbb{E}[\Gamma_{\text{PEC}}(\omega)^2] \leq \exp(2\gamma'r + \tilde{t}(e^{2\gamma c} - 1)). \quad (\text{C10})$$

Combining with the RLCU overhead bound yields

$$\epsilon^2 \leq \frac{1}{M} \exp\left(\frac{\tilde{t}^2}{r} + 2\gamma'r + \tilde{t}(e^{2\gamma c} - 1)\right), \quad (\text{C11})$$

which proves (58).  $\square$

## Appendix D: Derivation of the segmented SNI scaling

### 1. Setup and notation

We partition the  $d$ -layer Trotter circuit into  $s$  segments of equal depth  $d/s$ . Each segment contains  $dL/s$  elementary gates. Let  $q \leq 1 - (1 - \gamma)^L \simeq \gamma L$  denote the error probability per layer, where  $\gamma$  is the per-gate error rate. Under the stochastic Pauli noise assumption obtained via twirling, the per-segment error probability satisfies the bound

$$q_{\text{ST}} \leq \frac{qd}{s}. \quad (\text{D1})$$

The SNI method is applicable when  $q_{\text{ST}} < 1/2$ , which requires  $s > 2qd$ .

Applying SNI independently to each segment, the total sampling overhead is  $(1 - 2q_{\text{ST}})^{-2s}$ , and the number of samples required for the error-mitigated computation satisfies Eq. (78). The noise-characterization cost for estimating  $q_{\text{ST}}$  at each of the  $s$  segments is

$$M_{q_{\text{ST}}} = O(\epsilon^{-2} s^2 (1 - 2q_{\text{ST}})^{-4}), \quad (\text{D2})$$

where the factor  $s^2$  arises from requiring per-segment accuracy  $\epsilon/s$  to ensure overall accuracy  $\epsilon$  via the union bound.

### 2. Bounding the total overhead

We derive an upper bound on the per-segment overhead  $(1 - 2q_{\text{ST}})^{-s}$ . Taking the natural logarithm and applying the inequality  $-\ln(1 - x) \leq \frac{x}{1-x}$  for  $0 < x < 1$  with  $x = 2q_{\text{ST}}$ ,

$$\ln(1 - 2q_{\text{ST}})^{-s} = -s \ln(1 - 2q_{\text{ST}}) \leq \frac{2s q_{\text{ST}}}{1 - 2q_{\text{ST}}}. \quad (\text{D3})$$

The function  $g(y) = \frac{2y}{1-2y}$  is monotone increasing for  $0 < y < 1/2$ . Because  $q_{\text{ST}} \leq qd/s$  from Eq. (D1), substituting the upper bound gives

$$\frac{2s q_{\text{ST}}}{1 - 2q_{\text{ST}}} \leq \frac{2s \cdot (qd/s)}{1 - 2(qd/s)} = \frac{2qd}{1 - 2qd/s}. \quad (\text{D4})$$

Exponentiating yields the upper bound

$$(1 - 2q_{\text{ST}})^{-s} \leq \exp\left(\frac{2qd}{1 - 2qd/s}\right). \quad (\text{D5})$$

## Appendix E: Bounding the bias of the expectation values under noise and PEC

Let  $\{\mathcal{U}_k\}_{k=1}^{N_G}$  denote the ideal unitary channels implementing the target circuit, and let  $\{\mathcal{E}_k\}_{k=1}^{N_G}$  be noise channels. Note that we later consider the cases where  $\mathcal{E}_k$  is a simple error described by the CPTP channel and the  $\mathcal{E}_k$  corresponds to the residual error due to the incomplete noise characterization for PEC. Define

$$\mathcal{C}_{\text{noisy}} := \prod_{k=1}^{N_G} \mathcal{E}_k \mathcal{U}_k, \quad \mathcal{C}_{\text{ideal}} := \prod_{k=1}^{N_G} \mathcal{U}_k, \quad (\text{E1})$$

where  $\prod_{k=1}^{N_G} \mathcal{A}_k := \mathcal{A}_{N_G} \circ \dots \circ \mathcal{A}_1$ . We measure deviations with the channel distance

$$D(\mathcal{E}, \mathcal{F}) := \frac{1}{2} \|\mathcal{E} - \mathcal{F}\| \quad (\text{E2})$$

induced by a submultiplicative norm  $\|\cdot\|$  satisfying  $\|\Lambda \circ \Gamma\| \leq \|\Lambda\| \|\Gamma\|$  and  $\|\mathcal{U}\| = 1$  for any unitary channel  $\mathcal{U}$  (e.g., the diamond norm or an induced trace distance norm).

Setting  $\Phi_k := \mathcal{E}_k \circ \mathcal{U}_k$  and  $\Psi_k := \mathcal{U}_k$ , a telescoping identity gives

$$\prod_{k=1}^{N_G} \Phi_k - \prod_{k=1}^{N_G} \Psi_k = \sum_{j=1}^{N_G} \left( \prod_{k=j+1}^{N_G} \Phi_k \right) \circ (\Phi_j - \Psi_j) \circ \left( \prod_{k=1}^{j-1} \Psi_k \right). \quad (\text{E3})$$

Applying the triangle inequality and submultiplicativity yields the general bound

$$D(\mathcal{C}_{\text{noisy}}, \mathcal{C}_{\text{ideal}}) \leq \sum_{j=1}^{N_G} \left( \prod_{k=j+1}^{N_G} \|\mathcal{E}_k\| \right) D(\mathcal{E}_j, \mathcal{I}). \quad (\text{E4})$$

*Ordinary CPTP noise.* With no error mitigation, set  $\mathcal{E}_k = \mathcal{N}_k$  where each  $\mathcal{N}_k$  is a CPTP gate noise channel. Introducing the per-gate noise strength and norm,

$$\gamma := \max_k D(\mathcal{N}_k, \mathcal{I}), \quad M_{\text{noise}} := \max_k \|\mathcal{N}_k\|, \quad (\text{E5})$$

Eq. (E4) gives  $D(\mathcal{C}_{\text{noisy}}, \mathcal{C}_{\text{ideal}}) \leq \gamma \sum_{m=0}^{N_G-1} M_{\text{noise}}^m$ . For the diamond norm or an induced  $1 \rightarrow 1$  norm, CPTP maps satisfy  $M_{\text{noise}} = 1$ , yielding the linear accumulation bound

$$D(\mathcal{C}_{\text{noisy}}, \mathcal{C}_{\text{ideal}}) \leq N_G \gamma. \quad (\text{E6})$$

*Residual noise after PEC.* When probabilistic error cancellation is applied using an estimated noise model  $\{\mathcal{N}'_k\}$ , the effective channel on gate  $k$  becomes  $\mathcal{N}'_k{}^{-1} \circ \mathcal{N}_k \circ \mathcal{U}_k$ . The residual perturbation channel is therefore

$$\Delta \mathcal{N}_k := \mathcal{N}'_k{}^{-1} \circ \mathcal{N}_k. \quad (\text{E7})$$

Setting  $\mathcal{E}_k = \Delta \mathcal{N}_k$  in Eq. (E4) and introducing

$$\Delta \gamma := \max_{1 \leq k \leq N_G} D(\Delta \mathcal{N}_k, \mathcal{I}), \quad (\text{E8})$$

Eq. (E4) implies the uniform bound

$$D(\mathcal{C}_{\text{noisy}}, \mathcal{C}_{\text{ideal}}) \leq \Delta \gamma \sum_{j=1}^{N_G} \prod_{k=j+1}^{N_G} \|\Delta \mathcal{N}_k\|. \quad (\text{E9})$$

Letting  $M_\Delta := \max_k \|\Delta \mathcal{N}_k\|$ , Eq. (E9) gives

$$D(\mathcal{C}_{\text{noisy}}, \mathcal{C}_{\text{ideal}}) \leq \Delta \gamma \sum_{m=0}^{N_G-1} M_\Delta^m = \Delta \gamma \frac{M_\Delta^{N_G} - 1}{M_\Delta - 1}, \quad (M_\Delta \neq 1). \quad (\text{E10})$$

In the small-residual regime relevant to PEC,  $\|\Delta \mathcal{N}_k - \mathcal{I}\| \ll 1$  implies

$$\|\Delta \mathcal{N}_k\| \leq \|\mathcal{I}\| + \|\Delta \mathcal{N}_k - \mathcal{I}\| = 1 + 2D(\Delta \mathcal{N}_k, \mathcal{I}) \leq 1 + 2\Delta \gamma. \quad (\text{E11})$$

Substituting into Eq. (E9) gives

$$D(\mathcal{C}_{\text{noisy}}, \mathcal{C}_{\text{ideal}}) \leq \Delta \gamma \sum_{m=0}^{N_G-1} (1 + 2\Delta \gamma)^m = \frac{(1 + 2\Delta \gamma)^{N_G} - 1}{2}. \quad (\text{E12})$$

For  $\Delta \gamma \ll 1$ , expanding Eq. (E12) yields

$$D(\mathcal{C}_{\text{noisy}}, \mathcal{C}_{\text{ideal}}) = N_G \Delta \gamma + O(N_G^2 \Delta \gamma^2), \quad (\text{E13})$$

so the circuit-level deviation scales approximately linearly with the number of gates. In the regime of interest where the bias is small, the leading term dominates.

*Bounding  $\Delta\gamma$  via GST.* Let  $\Delta\gamma'_g := \max_k D(\mathcal{N}_k, \mathcal{N}'_k)$  denote the per-gate characterization error, and suppose  $D(\mathcal{N}'_k, \mathcal{I}) < \mu$  for all  $k$ . Because  $\mathcal{N}'_k{}^{-1} \circ \mathcal{N}'_k = \mathcal{I}$ , for each  $k$ ,

$$\begin{aligned} D(\Delta\mathcal{N}_k, \mathcal{I}) &= D(\mathcal{N}'_k{}^{-1} \circ \mathcal{N}_k, \mathcal{N}'_k{}^{-1} \circ \mathcal{N}'_k) \\ &= \frac{1}{2} \|\mathcal{N}'_k{}^{-1} \circ (\mathcal{N}_k - \mathcal{N}'_k)\| \leq \|\mathcal{N}'_k{}^{-1}\| D(\mathcal{N}_k, \mathcal{N}'_k). \end{aligned} \quad (\text{E14})$$

Because  $\|\mathcal{N}'_k - \mathcal{I}\| = 2D(\mathcal{N}'_k, \mathcal{I}) < 2\mu$ , a Neumann series argument gives, for  $\mu < 1/2$ ,

$$\|\mathcal{N}'_k{}^{-1}\| = \|(\mathcal{I} + (\mathcal{N}'_k - \mathcal{I}))^{-1}\| \leq \frac{1}{1 - \|\mathcal{N}'_k - \mathcal{I}\|} \leq \frac{1}{1 - 2\mu}. \quad (\text{E15})$$

Therefore,

$$\Delta\gamma \leq \frac{\Delta\gamma'_g}{1 - 2\mu}, \quad (\mu < \frac{1}{2}). \quad (\text{E16})$$

Because GST with  $M_g$  samples achieves  $\Delta\gamma'_g = O(1/\sqrt{M_g})$ , we obtain  $\Delta\gamma = O(1/\sqrt{M_g})$ . Combined with the leading-order bound, the bias in the expectation value satisfies

$$|\text{Bias}(\hat{\mu})| = |\text{Tr}[O \mathcal{C}_{\text{noisy}}(\rho)] - \text{Tr}[O \mathcal{C}_{\text{ideal}}(\rho)]| = O\left(\frac{N_G}{\sqrt{M_g}}\right) \quad (\text{E17})$$

for any observable  $O$  with  $\|O\|_\infty \leq 1$ .

For the randomized LCU algorithm,  $\mathcal{C}_{\text{noisy}}$  and  $\mathcal{C}_{\text{ideal}}$  are randomly generated circuits, and the same argument applies. The estimator involves reweighting by the sampling overhead  $\Gamma_{\text{RLCU}}$ , so the bias bound becomes  $\Gamma_{\text{RLCU}} N_G \Delta\gamma$  without error mitigation and  $\Gamma_{\text{RLCU}} N_G \Delta\gamma$  after PEC.